Title

Electrophysiological Phenotype in Angelman Syndrome Differs Between Genotypes

Journal

Biological Psychiatry, 85(9)

ISSN

0006-3223

Authors

Frohlich, Joel

Miller, Meghan T

Bird, Lynne M

et al.

Publication Date

2019-05-01

DOI

10.1016/j.biopsych.2019.01.008

HHS Public Access

Author manuscript

Biol Psychiatry. Author manuscript; available in PMC 2020 May 01.

Published in final edited form as:

Biol Psychiatry. 2019 May 01; 85(9): 752–759. doi:10.1016/j.biopsych.2019.01.008.

Electrophysiological phenotype in Angelman syndrome differs between genotypes

Joel Frohlich[1,2,*], **Meghan Miller**[1], **Lynne M. Bird**[3], **Pilar Garces**[1], **Hannah Purtell**[4], **Marius C. Hoener**[1], **Benjamin D. Philpot**[5], **Michael S. Sidorov**[5], **Wen-Hann Tan**[6], **Maria-Clemencia Hernandez**[1], **Alexander Rotenberg**[4], **Shafali S. Jeste**[2], **Michelle Krishnan**[1], **Omar Khwaja**[1], and **Joerg F. Hipp**[1,*]

[1]Roche Pharma Research and Early Development, Neuroscience, Ophthalmology and Rare Diseases, Roche Innovation Center Basel, Switzerland [2]Center for Autism Research and Treatment University of California, Los Angeles Semel Institute for Neuroscience, USA [3]Department of Pediatrics, University of California, San Diego; Genetics / Dysmorphology, Rady Children's Hospital San Diego, California, USA [4]Department of Neurology, Boston Children's Hospital; Harvard Medical School, Boston, Massachusetts, USA [5]Neuroscience Center, Carolina Institute for Developmental Disabilities, and Department of Cell Biology & Physiology, University of North Carolina, Chapel Hill, NC, USA [6]Division of Genetics and Genomics, Boston Children's Hospital; Harvard Medical School, Boston, Massachusetts, USA

Abstract

Background: Angelman syndrome is a severe neurodevelopmental disorder caused by either disruptions of the gene *UBE3A* or deletion of chromosome 15 at 15q11-q13, which encompasses *UBE3A* and several other genes, including *GABRB3*, *GABRA5*, *GABRG3* encoding GABA type-A receptor ($GABA_AR$) subunits (β3, α5, γ3). Individuals with deletions are generally more impaired than those with other genotypes, but the underlying pathophysiology remains largely unknown. Here we used electroencephalography (EEG) to test the hypothesis that genes other than *UBE3A* located on 15q11-q13 cause differences in pathophysiology between AS genotypes.

Methods: We compared spectral power of clinical EEG recordings from children (age: 1 – 18 years) with a deletion genotype ($n = 37$), a non-deletion genotype ($n = 21$), and typically developing children without Angelman syndrome ($n = 48$).

*Correspondence to: joelfrohlich@gmail.com, joerg.hipp@roche.com.

Joerg F. Hipp, Roche Pharma Research and Early Development, Neuroscience, Ophthalmology and Rare Diseases, Roche Innovation Center Basel, Grenzacherstrasse 124, CH-4070 Basel, Switzerland; joerg.hipp@roche.com; Phone: +41-6168-22382

ClinicalTrials.gov identifier: NCT00296764

Disclosures

Pilar Garces, Maria-Clemencia Hernandez, Joerg F. Hipp, Marius Hoener, Omar Khwaja, Michelle Krishnan and Meghan Miller are full-time employees of F. Hoffmann-La Roche Ltd.; Joel Frohlich is a former employee of F. Hoffmann-La Roche Ltd. (until July 2017); Shafali Jeste, Benjamin Philpot, and Alexander Rotenberg serve as a consultants for and have received funding from F. Hoffmann-La Roche Ltd.. All other authors report no biomedical financial interests or potential conflicts of interest.

Results: We found elevated theta power (peak frequency: 5.3 Hz) and diminished beta power (peak frequency: 23 Hz) in the deletion genotype compared to the non-deletion genotype, as well as excess broadband EEG power (1-32 Hz) peaking in the delta frequency range (peak frequency: 2.8 Hz) shared by both genotypes but stronger for the deletion genotype at younger ages.

Conclusions: Our results provide strong evidence for the contribution of non-UBE3A neuronal pathophysiology in deletion AS and suggest that hemizygosity of the *GABRB3-GABRA5-GABRG3* gene cluster causes abnormal theta and beta EEG oscillations that may underlie the more severe clinical phenotype. Our work improves the understanding of AS pathophysiology and has direct implications for the development of AS treatments and biomarkers.

Keywords

Angelman syndrome; EEG; GABA; UBE3A; biomarkers; GABRB3-GABRA5-GABRG3 gene cluster

Introduction

Angelman syndrome (AS) is a rare genetic neurodevelopmental disorder with a prevalence of 1 in 10,000–24,000 births (1, 2). Clinical traits of AS include global developmental delay, intellectual disability, microcephaly, epilepsy, sleep difficulties, and some phenotypic overlap with autism (3–6). The lack of functional UBE3A in neurons underlies core features of AS as evidenced by the phenotype of individuals with point mutations solely affecting this gene (7–9). UBE3A is a ubiquitin-protein ligase which is encoded by the eponymous gene *UBE3A* on chromosome 15 and is generally expressed only from the maternal allele in neurons but biallelically expressed in other cell types (8, 10, 11). The downstream consequences of UBE3A dysfunction are not understood in detail, but pre-clinical mouse models of AS show altered dendritic spine morphology (12, 13) and impaired synaptic function (14–17) that may underlie global electrophysiological abnormalities of the electroencephalography (EEG) (15, 18, 19). These pre-clinical findings are in line with neuropathological case studies in individuals with AS that point to cellular abnormalities in cortical pyramidal neurons including irregular distribution, decreased dendritic arborization, a reduced number of dendritic spines (20, 21), and a strongly abnormal EEG in AS (18, 22–24). Despite these anomalies, the gross anatomy is not particularly abnormal (25).

The etiology of AS can be divided into two broad groups (Fig. 1). The first group, “non-deletion AS”, mainly affects the function of UBE3A. Non-deletion AS, comprising 25–30% of all AS cases, includes *UBE3A* mutations, imprinting defects, and paternal uniparental disomy (UPD) (7, 26). The second group, “deletion AS”, is defined by deletions of chromosome 15 at 15q11-q13. Deletions vary in length (7) but all encompass *UBE3A*, as well as about 11–15 other protein-coding genes, numerous small nucleolar RNA (snoRNA) genes, and non-coding regions of potential functional significance. Deletion AS accounts for the majority (about 70%) of AS cases (7). Herein, we use “genotype” to refer to the two etiological groups defined above.

Individuals with deletion AS have a more severe clinical presentation than those with non-deletion AS (27–30), suggesting that deletion of genes other than *UBE3A* add to disease

severity. However, differences in the pathophysiology between AS genotypes remain largely unknown. Deletions of 15q11-q13 include the *GABRB3–GABRA5–GABRG3* gene cluster, which encodes the β3, α5, and γ3 $GABA_A$ receptor subunits. Given the important role of the GABAergic system in brain development and function, the deleted $GABA_AR$ subunit genes may cause important differences in AS genotypes. Indeed, several lines of evidence support this notion: (A) Mice with disruptions of *Gabrb3* recapitulate AS-like phenotypes (including seizures and EEG abnormalities) (31). (B) Deletion AS shows both altered cortical expression of the three $GABA_AR$ subunit genes (32) and reduced cortical $GABA_AR$ density (33) while also exhibiting grossly abnormal somatosensory evoked responses that may relate to GABAergic dysfunction (34). (C) Dup15q syndrome (a neurodevelopmental disorder characterized by intellectual disability, autism and epilepsy) is caused by duplications of 15q11.2-q13.1 (i.e., the "genetic converse" of deletion AS) and has a strong EEG phenotype characterized by excessive beta oscillations (35). These oscillations closely resemble the EEG signature of $GABA_AR$ enhancing drugs (e.g., benzodiazepines) (36), thereby implicating the *GABRB3-GABRA5-GABRG3* gene cluster in the Dup15q syndrome pathology and phenotype.

Given that the GABA system is critically involved in shaping neuronal dynamics, including oscillatory processes (37–39), EEG should provide a suitable tool to capture $GABA_AR$-related abnormalities in deletion AS.

AS is characterized by a strongly abnormal EEG (18, 22–24). Vendrame and colleagues (23) described EEG abnormalities in a large sample of 115 individuals with AS (here we analyze a subset of these individuals, see Methods) and found intermittent rhythmic delta oscillations (83.5%), interictal epileptiform discharges (74.2%), intermittent rhythmic theta oscillations (43.5%), and posterior rhythm slowing (43.5%). More recently, Sidorov and colleagues used quantitative analyses of AS EEGs and demonstrated excess power in the delta frequency band (18). However, these AS EEG abnormalities have been reported for both deletion and non-deletion AS genotypes. Comparing EEG differences between deletion and non-deletion AS may provide valuable insights into the respective contributions of *UBE3A* and non-*UBE3A* neuronal pathophysiology, but have not yet been quantitatively investigated.

Here we compared EEG power spectra between deletion and non-deletion AS. Considering the foregoing evidence, we tested two specific hypotheses concerning deletion AS compared to non-deletion AS: (A) stronger power in the delta frequency band and (B) weaker power in the beta frequency band, i.e., the opposite of the EEG phenotype observed in both Dup15q syndrome (35) and healthy individuals challenged with positive $GABA_AR$ modulators (36). We then explored a broad range of EEG frequencies in a data-driven manner.

Methods and Materials

See Supplemental Methods and Materials for an extended description of the methods.

Data Collection

EEG recordings were obtained from patients with AS through the AS Natural History Study (ClinicalTrials.gov identifier: NCT00296764; a subset of the data has been analyzed

previously (18, 23), see Supplemental Methods for more information). EEG recordings from a control group of children with typical development (TD) who had tested negative for neurological or developmental concerns were obtained through BCH. Consent was obtained according to the Declaration of Helsinki and was approved by the institutional review boards of the participating sites. EEG data were acquired in a clinical setting using an international 10-20 system. Data presented here are from children and adolescents, i.e., participants with ages between 12 – 216 months (1 – 18 years) recorded in the awake state. The awake state was not further controlled with respect to eye condition (e.g., eyes open or eyes closed) as the ages and developmental abilities of many participants precluded complying with such instructions. A total of 144 datasets entered preprocessing.

Preprocessing

EEG data were bandpass filtered 0.5 – 45 Hz (FIR filter), then portions of the data containing gross artifacts, as well as bad channels, were identified by visual inspection and excluded from analysis. Ten datasets were excluded for overall insufficient data quality. Independent component analysis (ICA) was applied to remove remaining artifacts (FastICA algorithm (40, 41)). Finally, rejected channels were interpolated and data were re-referenced to average. The final dataset analyzed included 127 recordings from 106 participants. The average individual dataset length was 15.9 ± 8.36 minutes (mean ± std). See Supplemental Table 1 for a summary of retained data by genotype and testing site.

Frequency Transform

Power spectral estimates were derived for logarithmically scaled frequencies ranging from 1 to 32 Hz ($f/\sigma_f = 8.7$) using Morlet Wavelets (42). Absolute power values were then scaled and log-transformed to have units $10*\log_{10}(\mu V^2/\log_2(Hz))$. Consequently, differences between signals have the unit decibel (dB). For analyses of relative power, data were expressed in units of $1/\log_2(Hz)$.

Peak frequencies

Peak frequencies were determined within pre-defined frequency ranges (delta: 1.5–4 Hz; theta 4–8 Hz). Additionally, we reported the “center of mass”, derived as the weighted average value of the frequency within the two frequency ranges.

Statistical analyses

For statistical analysis, we used the following linear mixed model (LMM) (43) and variants with less fixed factors:

$$P \sim 1 + GENOTYPE + AGE + GENOTYPE:AGE + (1 \mid PARTICIPANT)$$

where P is log-transformed power in a given frequency band, AGE is the $\log_2$-transformed and mean-centered age, and GENOTYPE contains categorical variables [AS, TD], [deletion, non-deletion], or [deletion class I, deletion class II].

To derive 95% confidence intervals for illustration, and to test specific hypotheses, we used t-tests within LMMs. To test for relevance of factors (e.g. GENOTYPE or AGE), we used

log-likelihood ratio tests between nested models. To correct for multiple comparisons when performing analyses across all frequencies, we additionally applied a random permutation approach (44). Finally, to evaluate stability of the delta-band EEG power we used the intraclass correlation coefficient (ICC) derived from the first two visits of participants with more than one visit (45).

Results

We obtained clinical EEG data in the awake state from children and adolescents (1 to 18 years of age) with AS and TD controls. After preprocessing and quality control, we retained 49 datasets from 37 individuals (10 females) with deletion AS, 30 datasets from 21 individuals (6 females) with non-deletion AS, and single-visit datasets from 48 TD controls (22 females, Fig. 1). There is an over-representation of males in the AS sample that is close to significance compared to TD controls ($p = 0.054$, Chi-Square test). This is likely due to chance given that AS is an autosomal disorder with no known difference in prevalence between genders. Importantly, the gender ratio did not differ between AS genotypes ($p = 0.90$, Chi-Square test). In line with previous reports, participants with AS presented with global developmental delay, lack of speech, and epilepsy (See Supplemental Fig. 1). Mean age (deletion AS: 4.6 ± 3.0, non-deletion AS, 7.3 ± 3.3, TD controls: 8.8 ± 5.0; mean ± std in years, age averaged across multiple visits) differed significantly between AS genotypes ($p = 1.66 \times 10^{-4}$) and between AS and TD cohorts ($p = 2.50 \times 10^{-3}$). Age was accounted for in the subsequent analyses.

Spectral power differs between AS and TD controls

We first investigated differences in EEG spectral power between AS (combined deletion and non-deletion genotypes) and TD controls. For each visit of each participant, we derived spectral power estimates (1 to 32 Hz), averaged across electrodes, and fitted LMMs for each frequency separately (see methods). To test for differences between participants with AS and TD controls, we compared the model to a nested model lacking diagnosis (AS, TD) information. Importantly, the models accounted for age and repeated visits of the same individuals. We found that spectral power differed between AS and TD controls for all frequencies (i.e., AS vs TD labels significantly contributed to the model fit; $p < 0.05$, random permutation test, corrected for all frequencies).

To understand the directionality of the difference in spectral power, we set the age in the model to the mean log age (5.4 years) and investigated group differences. We found higher power for AS compared to TD controls across all frequencies (Fig. 2A, Supplemental Fig. 2A). The largest difference manifested in a prominent peak in the delta frequency range (peak frequency = 2.8 Hz, Cohen's $d = 1.22$, power difference AS vs TD: 11.1 dB or 1182%). Excess power in the delta frequency was a global phenomenon visible at all electrodes, demonstrating the largest effect size at temporal electrodes (Fig. 2B,C, Supplemental Fig. 2B). A total of 16 AS participants had at least two separate EEG assessments (12.9 ± 3.11 months apart) allowing us to investigate stability. The delta-band EEG power had moderate stability (ICC: 0.68; see Supplemental Figure 2C). While excess power was most prominent in the delta frequency range, power was broadly elevated.

Testing total power (i.e., integrating power over all frequencies) yielded a similar effect size between AS and TD (Supplemental Table 2 for full details, Supplemental Fig. 2D).

It is well established in typical development that absolute EEG power at all frequencies decreases, while the relative power at higher frequencies (> 8 Hz) increases, with age (46, 47). We next investigated the developmental trajectory of AS delta power in terms of both power and peak frequency, i.e., the two key quantities characterizing oscillatory processes. Power at the AS group-level delta peak frequency exhibited a significant decline with age in both groups (Fig. 2D, TD: −3.17 dB/oct, $p = 0.385 \times 10^{-7}$; AS: −4.20 dB/oct, $p = 4.21 \times 10^{-12}$, LMM parameters in Supplemental Table 3 for full details). Slopes did not differ significantly between AS and TD controls (Difference: −1.03 dB/oct, p = 0.202). Clear delta peaks could be identified in 70 EEG recordings from 54 out of 58 participants with AS (Supplemental Fig. 5A). The delta peak frequency was not associated with age (LMM, log-likelihood ratio test of model with and without age, p = 0.492). Center of mass, an alternative metric for quantifying the dominant frequency, also showed no relationship with age (frequency range: 1.5 – 4 Hz, p = 0.832). Thus, the excess EEG delta power in AS decreases during development at a similar rate as TD controls and consequently remains at a higher baseline throughout development.

Excess power in the delta frequency range is in line with previous reports of excess relative delta power in AS compared to TD controls (18). Our results show that power is increased across all frequencies analyzed (1-32 Hz) and exhibits the strongest difference in the delta frequency range. Consequently, the effect size is larger for absolute power compared to relative power (absolute power: Cohen's d = 1.22, relative power: Cohen's d = 0.67, at delta peak frequency, 2.8 Hz; see Supplemental Fig. 3 for the analysis of relative power).

Spectral power differs between AS genotypes

To investigate phenotypic differences in EEG spectral power between AS subtypes, we split the AS group into deletion AS ($n = 34$, participants with class I or class II deletion) and non-deletion AS ($n = 21$) subgroups. First, we tested the two specific hypotheses as outlined in the introduction. A comparison of delta power between AS deletion genotypes (hypothesis 1) at the AS group level peak frequency (2.8 Hz) revealed 2.97 dB higher power compared to the AS non-deletion genotype at mean log age of 4.7 years (corresponding to 198.3% power relative to non-deletion AS; Fig. 3A; $p = 0.0498$, two-tailed t-test, LMM parameters in Supplemental Table 4 for full details). The power differences decline with age and were greatest over temporal scalp regions (Fig. 3B,C). A comparison of beta power in AS deletion genotypes at the Dup15q syndrome peak frequency (hypothesis 2; 23 Hz (35)) revealed −1.69 dB lower power compared to non-deletion AS at mean log age of 4.7 years (corresponding to 67.7% relative to non-deletion AS; Fig. 4A; p = 0.0168, two-tailed t-test, LMM parameter in Supplemental Table 5 for full details). Power differences at 23 Hz were greatest over central scalp regions (Fig 4B,C). Thus, the AS deletion genotype exhibits stronger delta power but weaker beta power than the non-deletion AS genotype. The latter observation in the AS deletion genotype resembles an inversion of the Dup15q syndrome EEG phenotype (35).

Next, we switched to an exploratory analysis and tested for AS genotype differences in an unbiased and data-driven manner across the full frequency range. This analysis revealed highly significant excess theta-band power of 5.20 dB centered at 5.3 Hz for deletion AS compared to non-deletion AS (corresponding to 331% of the non-deletion AS value; Fig. 5A,B, Supplemental Fig. 4A-C; $p < 0.01$, LMM-based random permutation test corrected for multiple comparisons across frequencies and accounting for age, LMM parameter for 5.3 Hz in Supplemental Table 6). A local maximum existed in theta-band only for deletion AS but not for non-deletion AS. Power differences in 5.3 Hz power were greatest over centro-temporal regions (Fig. 5E-G). In sum, these results suggest that the EEG phenotype of deletion AS is characterized by an oscillation in the theta frequency range that is absent in non-deletion AS.

We then investigated the developmental trajectory of the theta-band deletion AS phenotype in terms of both power and peak frequency (Fig. 5C). We found a significant decrease in theta power (5.3 Hz) with age for deletion AS (slope −2.26 dB/oct, $p = 3.45 \times 10^{-4}$) but not for non-deletion AS (slope: −1.27 dB/oct, $p = 0.185$). This suggests a developmental decline of the deletion AS theta-band oscillation. However, slopes did not significantly differ between AS subgroups (difference in slope: −0.99 dB/oct, $p = 0.381$; see Supplemental Fig. 4E for topography).

Clear theta peaks could be identified in 37 EEG recordings from 28 of 34 participants with class I or class II deletion AS (participants with atypical deletions were excluded; Supplemental Fig. 5B). For participants with theta peaks, we found a significant increase of 0.31 dB/oct in peak frequency with age (LMM, log-likelihood ratio test of model with and without age, $p = 0.011$; Fig. 5D). This finding was confirmed using an alternative approach that quantifies the dominant frequency, i.e., center of mass, which can be derived for all deletion AS participants ($p = 8.70 \times 10^{-5}$, slope: 0.15 Hz/oct, see Supplemental Fig. 4D). Thus, the deletion AS theta oscillations increase in frequency over the course of development.

The deletion group can be further broken down into subgroups with different deletion size (class I: ~6Mb; class II: ~5 Mb; we excluded rare atypical deletions from analysis (7, 48)). However, we did not find an improved model fit when adding deletion subclass information, even when ignoring the correction for multiple testing across frequencies ($p > 0.05$, log-likelihood ratio tests). Notably, both deletion subgroups encompass the *GABRB3-GABRA5-GABRG3* gene cluster. This suggests that the genes responsible for driving the differences between deletion AS and non-deletion AS reside in the region shared by deletion classes 1 and 2.

To examine potential confounders introduced by medication, we categorized all medications taken by participants that either (A) act principally on the CNS or (B) have incidental CNS side effects. Medications were classified by a physician, and further subcategories were established for CNS medications: antiepileptics, antipsychotics, alpha agonists, and stimulants. For each category and subcategory, we calculated the proportion of participants in each AS genotype taking a medication during at least one EEG recording used in our analysis (Table 1 and Supplemental Fig. 6). Chi-squared tests did not reveal differences

between AS genotypes, suggesting that differences in EEG reflect differences in pathophysiology rather than medication.

Discussion

Our findings demonstrate a robust electrophysiological phenotype in children with AS and reveal several frequency-specific differences between deletion and non-deletion AS genotypes. In the following, we summarize phenotypic differences, link them to GABAergic signaling, and discuss practical implications for the use of EEG as a biomarker.

Excess delta-band oscillations are a robust UBE3A-related AS phenotype

We found excess delta oscillations to be the most prominent AS EEG phenotype. This result agrees with clinical observations of qualitatively abnormal EEG activity in AS (22, 49, 50) and a recent publication by Sidorov and colleagues that demonstrated a robust increase in relative power in the same frequency range (18). Our results extend previous work in several directions: (A) We showed that EEG power is elevated across a broad range of frequencies (i.e. all frequencies analyzed, 1 – 32 Hz) and, consequently, absolute delta power better separates AS and TD controls as compared to relative delta power. The origin of this frequency-unspecific increase of EEG signal power is unknown, and it is unclear if it relates to neurophysiological or, alternatively, anatomical abnormalities (e.g., altered tissue conductivities; though somatic and head growth are relatively normal in AS, see Supplemental Figure 1). (B) We characterized the developmental trajectory across a broad age range (1 – 18 years) and showed that delta power increase (relative to TD controls) is stable across development. (C) We found that the delta-band AS phenotype is more pronounced for deletion as compared to non-deletion AS at young ages, though future studies with better age-matched data at younger ages are needed to elaborate on this finding. (D) Finally, we showed the delta-band power increase in AS is wide-spread but strongest at temporal electrodes. The pathophysiological mechanisms underlying the delta-band EEG phenotype are unknown; nonetheless, our results provide some insights. The observation that the delta EEG phenotype is present in both deletion and non-deletion AS suggests that it is driven by down-stream effects of UBE3A disruption. For instance, tonic GABAergic inhibition impaired through disruption of UBE3A-dependent GAT1 degradation (51) might underlie the delta EEG phenotype. However, it is well established both preclinically (12–17) and clinically (20, 21) that the lack of UBE3A leads to cellular abnormalities and impaired synaptic function, which in turn may manifest in the observed abnormal delta activity.

Theta and beta-band oscillations index non-UBE3A pathophysiology in deletion AS implicating the GABRB3-GABRA5-GABRG3 gene cluster

First, we confirmed the hypothesis, put forward in the introduction, that beta-band power is decreased in deletion AS compared to non-deletion AS. This builds on recent work in Dup15q syndrome (35, 52) suggesting that EEG beta-band activity reflects a gene-dose effect of the three $GABA_AR$ subunit genes (*GABRA5, GABRB3*, and *GABRG3*) manifesting in altered $GABA_AR$ density and, consequently, in altered network dynamics. These changes in the beta frequency band likely reflect abnormalities in recurrent excitatory-inhibitory feedback loops in cortical tissue (53, 54) and are well in line with

pharmacological effects of $GABA_AR$ modulators (36). Notably, the spatial topography of the beta-band modulation in Dup15q syndrome and AS is very different (Fig. 4B,C, *c.f.* Fig. 2 in Frohlich and colleagues (35)). This may be expected if certain brain areas start from a state where beta oscillations can be upregulated, but not downregulated, while other brain areas start from a state where beta oscillations can be down-regulated, but not further upregulated. Although the cortical networks underlying our finding remain unknown, the observation of lower beta power in the deletion AS genotype nonetheless adds to the rationale for targeting $GABA_ARs$ in the group of neurodevelopmental disorders affecting the *GABRB3-GABRA5-GABRG3* gene cluster (e.g., AS, Prader-Will syndrome (PWS) and Dup15q syndrome).

The most prominent difference between AS genotypes, however, was not anticipated by our hypotheses: oscillatory activity in the theta frequency range, which is present only for the deletion AS genotype. Rhythmic theta in AS has been qualitatively described in previous publications (23, 24, 55, 56), but to the best of our knowledge, our work is the first to quantify excess theta oscillations and to link them to the deletion AS genotype. Given that $GABA_ARs$ are critically involved in shaping neuronal dynamics reflected in EEG oscillations (37–39), deletion of the *GABRB3-GABRA5-GABRG3* gene cluster is the most likely cause of the AS genotype differences observed in our study. However, we cannot rule out contributions from genes common to both deletions classes beyond the *GABRB3-GABRA5-GABRG3* gene cluster, though EEG effects related to these other genes are unknown. Other important 15q11-q13 genes that are not shared by the two major deletion classes (class I and class II), e.g., *CYFIP1*, can be effectively ruled out as explanations for the EEG effect within the limits of the statistical power of our study.

$GABA_AR$ hypothesis provides testable predictions

As outlined above, our results suggest that deletion of the *GABRB3-GABRA5-GABRG3* gene cluster underlies the electrophysiological differences between AS deletion and non-deletion genotypes. This $GABA_AR$ hypothesis provides specific, falsifiable predictions. For instance, our work makes testable predictions concerning EEG abnormalities that should be observable in Prader-Willi syndrome (PWS), a neurogenetic disorder caused by either a paternal 15q11-q13 deletion or maternal UPD of chromosome 15 (57), and suggests pre-clinical experiments in knock-out animals that investigate the effect of *Ube3a* and GABA-subunit gene loss in isolation and in combination (see Supplemental Discussion for more details).

EEG as a biomarker of AS

Understanding the AS EEG phenotype also has important practical implications for the development of treatments. For successful clinical development of a potential treatment, biomarkers that quantify the disease pathophysiology and provide an objective indicator of treatment response are of critical importance (58). EEG has been suggested as a promising quantitative, robust, and translatable biomarker for AS (18). Highly targeted AS treatments (e.g., antisense oligonucleotides) acting specifically on *UBE3A* expression (59–61) require biomarkers to demonstrate target engagement and treatment effects. Our findings provide evidence that the delta-band EEG abnormality indexes *UBE3A*-related pathophysiology, while the theta-band and beta-band EEG abnormalities index contributions from other genes,

most likely the *GABRB3-GABRA5-GABRG3* gene cluster. Thus, if re-expression of *UBE3A* is the main target of the treatment, EEG delta-band power should be explored as a biomarker, whereas if the $GABA_AR$s are the target, theta and beta power should be considered as a biomarkers.

Conclusions

Our results suggest that hemizygosity of genes encoding $GABA_AR$ subunits modulates the *UBE3A*-related electrophysiological phenotype and causes widespread changes in cortical dynamics, manifesting as spectrally specific abnormalities in oscillatory neuronal activity. These electrophysiological abnormalities may underlie the more severe behavioral phenotype of deletion AS. Our work has direct implications for the use of EEG as a biomarker in the development of treatments for AS.

Supplementary Material

Refer to Web version on PubMed Central for supplementary material.

Acknowledgments

We thank the children and families who participated in this study for their generosity. Our work would not be possible without their involvement. We are also indebted to Nima Chenari for contributing the artwork in Figure 1.

This study was supported by NIH U54RR019478 (awarded to Arthur Beaudet) and U54HD061222 (awarded to Alan Percy).

Dr. Rotenberg's research related to the present manuscript is supported by NIH NIMH R01MH100186, NIH NINDS R01NS088583, NIH NINDS R01NS100766 and the Translational Research Program at Boston Children's Hospital. Dr. Philpot's research was supported by NIH NICHD R01HD093771.

References

1. Mertz LGB, Christensen R, Vogel I, Hertz JM, Nielsen KB, Grønskov K, Østergaard JR (2013): Angelman syndrome in Denmark. Birth incidence, genetic findings, and age at diagnosis. American Journal of Medical Genetics Part A. 161: 2197–2203.
2. Petersen MB, Brøndum-Nielsen K, Hansen LK, Wulff K (1995): Clinical, cytogenetic, and molecular diagnosis of Angelman syndrome: estimated prevalence rate in a Danish county. American journal of medical genetics. 60: 261–262. [PubMed: 7573182]
3. Williams CA (1995): Angelman syndrome: consensus for diagnostic criteria. American journal of medical genetics. 56: 237–238. [PubMed: 7625452]
4. Trillingsgaard A, Østergaard JR (2004): Autism in Angelman syndrome: an exploration of comorbidity. Autism. 8: 163–174. [PubMed: 15165432]
5. Thibert RL, Larson AM, Hsieh DT, Raby AR, Thiele EA (2013): Neurologic manifestations of Angelman syndrome. Pediatric neurology. 48: 271–279. [PubMed: 23498559]
6. Bird LM (2014): Angelman syndrome: review of clinical and molecular aspects. The application of clinical genetics. 7: 93. [PubMed: 24876791]
7. Buiting K, Williams C, Horsthemke B (2016): Angelman syndrome—insights into a rare neurogenetic disorder. Nature Reviews Neurology. 12: nrneurol-2016.
8. Chamberlain SJ, Lalande M (2010): Angelman syndrome, a genomic imprinting disorder of the brain. Journal of Neuroscience. 30: 9958–9963. [PubMed: 20668179]
9. Kishino T, Lalande M, Wagstaff J (1997): UBE3A/E6-AP mutations cause Angelman syndrome. Nature genetics. 15: 70–73. [PubMed: 8988171]

10. Yamasaki K, Joh K, Ohta T, Masuzaki H, Ishimaru T, Mukai T, et al. (2003): Neurons but not glial cells show reciprocal imprinting of sense and antisense transcripts of Ube3a. Human molecular genetics. 12: 837–847. [PubMed: 12668607]
11. Albrecht U, Sutcliffe JS, Cattanach BM, Beechey CV, Armstrong D, Eichele G, Beaudet AL (1997): Imprinted expression of the murine Angelman syndrome gene, Ube3a, in hippocampal and Purkinje neurons. Nature genetics. 17: 75–78. [PubMed: 9288101]
12. Dindot SV, Antalffy BA, Bhattacharjee MB, Beaudet AL (2008): The Angelman syndrome ubiquitin ligase localizes to the synapse and nucleus, and maternal deficiency results in abnormal dendritic spine morphology. Hum Mol Genet. 17: 111–118. [PubMed: 17940072]
13. Kim H, Kunz PA, Mooney R, Philpot BD, Smith SL (2016): Maternal Loss of Ube3a Impairs Experience-Driven Dendritic Spine Maintenance in the Developing Visual Cortex. J Neurosci. 36: 4888–4894. [PubMed: 27122043]
14. Wallace ML, Burette AC, Weinberg RJ, Philpot BD (2012): Maternal Loss of Ube3a Produces an Excitatory/Inhibitory Imbalance through Neuron Type-Specific Synaptic Defects. Neuron. 74: 793–800. [PubMed: 22681684]
15. Judson MC, Wallace ML, Sidorov MS, Burette AC, Gu B, van Woerden GM, et al. (2016): GABAergic neuron-specific loss of Ube3a causes Angelman syndrome-like EEG abnormalities and enhances seizure susceptibility. Neuron. 90: 56–69. [PubMed: 27021170]
16. Yashiro K, Riday TT, Condon KH, Roberts AC, Bernardo DR, Prakash R, et al. (2009): Ube3a is required for experience-dependent maturation of the neocortex. Nature Neuroscience. 12: 777–783. [PubMed: 19430469]
17. Sato M, Stryker MP (2010): Genomic imprinting of experience-dependent cortical plasticity by the ubiquitin ligase gene Ube3a. PNAS. 107: 5611–5616. [PubMed: 20212164]
18. Sidorov MS, Deck GM, Dolatshahi M, Thibert RL, Bird LM, Chu CJ, Philpot BD (2017): Delta rhythmicity is a reliable EEG biomarker in Angelman syndrome: a parallel mouse and human analysis. Journal of neurodevelopmental disorders. 9: 17. [PubMed: 28503211]
19. Born HA, Dao AT, Levine AT, Lee WL, Mehta NM, Mehra S, et al. (2017): Strain-dependence of the Angelman Syndrome phenotypes in Ube3a maternal deficiency mice. Scientific Reports. 7: 8451. [PubMed: 28814801]
20. Kyriakides T, Hallam LA, Hockey A, Silberstein P, Kakulas BA (1992): Angelman's syndrome: a neuropathological study. Acta Neuropathol. 83: 675–678. [PubMed: 1636384]
21. Jay V, Becker LE, Chan FW, Perry TL (1991): Puppet-like syndrome of Angelman: a pathologic and neurochemical study. Neurology. 41: 416–422. [PubMed: 2006012]
22. Laan LA, Vein AA (2005): Angelman syndrome: is there a characteristic EEG? Brain and Development. 27: 80–87. [PubMed: 15668045]
23. Vendrame M, Loddenkemper T, Zarowski M, Gregas M, Shuhaiber H, Sarco DP, et al. (2012): Analysis of EEG patterns and genotypes in patients with Angelman syndrome. Epilepsy & Behavior. 23: 261–265. [PubMed: 22341959]
24. Dan B, Boyd S (2003): Angelman syndrome reviewed from a neurophysiological perspective. The UBE3A-GABRB3 hypothesis. Neuropediatrics. 34: 169–176. [PubMed: 12973656]
25. Harting I, Seitz A, Rating D, Sartor K, Zschocke J, Janssen B, et al. (2009): Abnormal myelination in Angelman syndrome. European Journal of Paediatric Neurology. 13: 271–276. [PubMed: 18573670]
26. Clayton-Smith J, Laan L (2003): Angelman syndrome: a review of the clinical and genetic aspects. Journal of medical genetics. 40: 87–95. [PubMed: 12566516]
27. Moncla A, Malzac P, Voelckel M-A, Auquier P, Girardot L, Mattei M-G, et al. (1999): Phenotype–genotype correlation in 20 deletion and 20 non-deletion Angelman syndrome patients. European Journal of Human Genetics. 7.
28. Lossie A, Whitney M, Amidon D, Dong H, Chen P, Theriaque D, et al. (2001): Distinct phenotypes distinguish the molecular classes of Angelman syndrome. Journal of medical genetics. 38: 834–845. [PubMed: 11748306]
29. Minassian BA, Delorey TM, Olsen RW, Philippart M, Bronstein Y, Zhang Q, et al. (1998): Angelman syndrome: correlations between epilepsy phenotypes and genotypes. Annals of neurology. 43: 485–493. [PubMed: 9546330]

30. Gentile JK, Tan W-H, Horowitz LT, Bacino CA, Skinner SA, Barbieri-Welge R, et al. (2010): A neurodevelopmental survey of Angelman syndrome with genotype-phenotype correlations. Journal of developmental and behavioral pediatrics: JDBP. 31: 592. [PubMed: 20729760]

31. DeLorey T, Handforth A, Anagnostaras S, Homanics G, Minassian B, Asatourian A, et al. (1998): Mice lacking the β3 subunit of the GABAA receptor have the epilepsy phenotype and many of the behavioral characteristics of Angelman syndrome. Journal of Neuroscience. 18: 8505–8514. [PubMed: 9763493]

32. Roden WH, Peugh LD, Jansen LA (2010): Altered GABAA receptor subunit expression and pharmacology in human Angelman syndrome cortex. Neuroscience letters. 483: 167–172. [PubMed: 20692323]

33. Holopainen IE, Metsähonkala EL, Kokkonen H, Parkkola RK, Manner TE, Någren K, Korpi ER (2001): Decreased binding of [11C]flumazenil in Angelman syndrome patients with GABA(A) receptor beta3 subunit deletions. Ann Neurol. 49: 110–113. [PubMed: 11198279]

34. Egawa K, Asahina N, Shiraishi H, Kamada K, Takeuchi F, Nakane S, et al. (2008): Aberrant somatosensory-evoked responses imply GABAergic dysfunction in Angelman syndrome. Neuroimage. 39: 593–599. [PubMed: 17962046]

35. Frohlich J, Senturk D, Saravanapandian V, Golshani P, Reiter LT, Sankar R, et al. (2016): A quantitative electrophysiological biomarker of duplication 15q11. 2-q13. 1 syndrome. PloS one. 11: e0167179. [PubMed: 27977700]

36. Greenblatt DJ, Ehrenberg BL, Gunderman J, Locniskar A, Scavone JM, Harmatz JS, Shader RI (1989): Pharmacokinetic and electroencephalographic study of intravenous diazepam, midazolam, and placebo. Clinical Pharmacology & Therapeutics. 45: 356–365. [PubMed: 2702793]

37. Wang X-J (2010): Neurophysiological and computational principles of cortical rhythms in cognition. Physiological reviews. 90: 1195–1268. [PubMed: 20664082]

38. Steriade M, Timofeev I (2003): Neuronal plasticity in thalamocortical networks during sleep and waking oscillations. Neuron. 37: 563–576. [PubMed: 12597855]

39. Womelsdorf T, Valiante TA, Sahin NT, Miller KJ, Tiesinga P (2014): Dynamic circuit motifs underlying rhythmic gain control, gating and integration. Nature neuroscience. 17: 1031. [PubMed: 25065440]

40. Hyvarinen A (1999): Fast ICA for noisy data using Gaussian moments. (Vol. 5), Presented at the Circuits and Systems, 1999. ISCAS'99. Proceedings of the 1999 IEEE International Symposium on, IEEE, pp 57–61.

41. Jung T-P, Makeig S, Westerfield M, Townsend J, Courchesne E, Sejnowski TJ (2000): Removal of eye activity artifacts from visual event-related potentials in normal and clinical subjects. Clinical Neurophysiology. 111: 1745–1758. [PubMed: 11018488]

42. Tallon-Baudry C, Bertrand O, Delpuech C, Pernier J (1997): Oscillatory γ-band (30–70 Hz) activity induced by a visual search task in humans. Journal of Neuroscience. 17: 722–734. [PubMed: 8987794]

43. West BT, results search, results search (2014): Linear Mixed Models: A Practical Guide Using Statistical Software, Second Edition, 2 edition. Boca Raton: Chapman and Hall/CRC.

44. Nichols TE, Holmes AP (2002): Nonparametric permutation tests for functional neuroimaging: a primer with examples. Human brain mapping. 15: 1–25. [PubMed: 11747097]

45. McGraw KO PS (1996): Forming inferences about some intraclass correlation coefficients. Psychological Methods. 1: 30–46.

46. Gasser T, Verleger R, Bächer P, Sroka L (1988): Development of the EEG of school-age children and adolescents. I. Analysis of band power. Electroencephalography and Clinical Neurophysiology. 69: 91–99. [PubMed: 2446839]

47. Marshall PJ, Bar-Haim Y, Fox NA (2002): Development of the EEG from 5 months to 4 years of age. Clinical Neurophysiology. 113: 1199–1208. [PubMed: 12139998]

48. Finucane BM, Lusk L, Arkilo D, Chamberlain S, Devinsky O, Dindot S, et al. (2016): 15q duplication syndrome and related disorders. .

49. Williams CA (2005): Neurological aspects of the Angelman syndrome. Brain and Development. 27: 88–94. [PubMed: 15668046]

50. Boyd S, Harden A, Patton M (1988): The EEG in early diagnosis of the Angelman (happy puppet) syndrome. European journal of pediatrics. 147: 508–513. [PubMed: 3409926]
51. Egawa K, Kitagawa K, Inoue K, Takayama M, Takayama C, Saitoh S, et al. (2012): Decreased Tonic Inhibition in Cerebellar Granule Cells Causes Motor Dysfunction in a Mouse Model of Angelman Syndrome. Science Translational Medicine. 4: 163ra157–163ra157.
52. Urraca N, Cleary J, Brewer V, Pivnick EK, McVicar K, Thibert RL, et al. (2013): The interstitial duplication 15q11.2-q13 syndrome includes autism, mild facial anomalies and a characteristic EEG signature. Autism Res. 6: 268–279. [PubMed: 23495136]
53. Jensen O, Goel P, Kopell N, Pohja M, Hari R, Ermentrout B (2005): On the human sensorimotor-cortex beta rhythm: Sources and modeling. NeuroImage. 26: 347–355. [PubMed: 15907295]
54. Whittington MA, Traub RD, Kopell N, Ermentrout B, Buhl EH (2000): Inhibition-based rhythms: experimental and mathematical observations on network dynamics. International Journal of Psychophysiology. 38: 315–336. [PubMed: 11102670]
55. Sugimoto T, Yasuhara A, Ohta T, Nishida N, Saitoh S, Hamabe J, Niikawa N (1992): Angelman syndrome in three siblings: characteristic epileptic seizures and EEG abnormalities. Epilepsia. 33: 1078–1082. [PubMed: 1464267]
56. Valente KD, Andrade JQ, Grossmann RM, Kok F, Fridman C, Koiffmann CP, Marques-Dias MJ (2003): Angelman syndrome: difficulties in EEG pattern recognition and possible misinterpretations. Epilepsia. 44: 1051–1063. [PubMed: 12887436]
57. Cassidy SB, Driscoll DJ (2009): Prader–Willi syndrome. European Journal of Human Genetics. 17: 3. [PubMed: 18781185]
58. Jeste SS, Frohlich J, Loo SK (2015): Electrophysiological biomarkers of diagnosis and outcome in neurodevelopmental disorders. Curr Opin Neurol. . doi: 10.1097/WCO.0000000000000181.
59. Matsuura T, Sutcliffe JS, Fang P, Galjaard R-J, Jiang Y, Benton CS, et al. (1997): De novo truncating mutations in E6-AP ubiquitin-protein ligase gene (UBE3A) in Angelman syndrome. Nature genetics. 15: 74. [PubMed: 8988172]
60. Meng L, Ward AJ, Chun S, Bennett CF, Beaudet AL, Rigo F (2015): Towards a therapy for Angelman syndrome by targeting a long non-coding RNA. Nature. 518: 409–412. [PubMed: 25470045]
61. Bishop KM (2017): Progress and promise of antisense oligonucleotide therapeutics for central nervous system diseases. Neuropharmacology. 120: 56–62. [PubMed: 27998711]

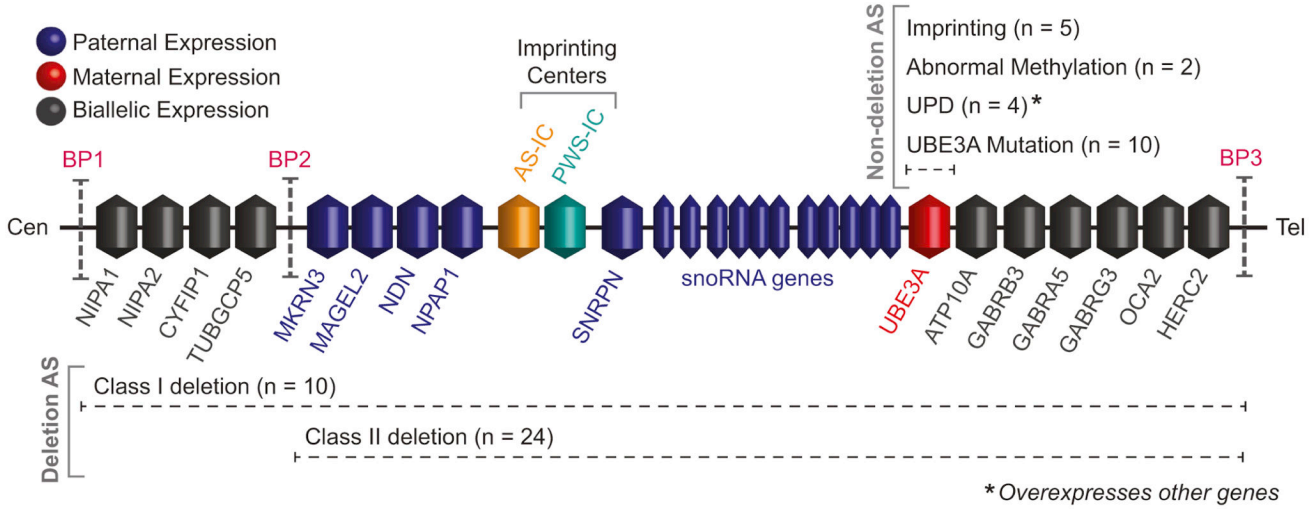

Figure 1. Schematic of 15q11-q13.

The maternally expressed (i.e., paternally imprinted in neurons) gene UBE3A is shown in red, paternally expressed (i.e., maternally imprinted in neurons) genes are shown in blue. Genes shown in black are non-imprinted (i.e., biallelically expressed); "n" indicates the number of participants for different genotypes. UBE3A mutations (n = 10), paternal UPD (n = 4), imprinting defects (n = 5; could either be deletion within the imprinting center or an abnormal epigenetic imprint), and abnormal DNA methylation that are not deletions (could be either UPD or imprinting defects, n = 2) primarily affect UBE3A. These etiologies comprise the non-deletion genotype (n = 21) in our study. Note that UPD features additionally biallelic expression of paternally imprinted genes (blue). Deletions of 15q11-q13 are typically between canonical break point (BPs) as indicated in the figure. Class I is a ~6 Mb deletion from BP 1 to BP3 (n = 10) that includes four additional genes near the centromere as compared with class II (~5 Mb) deletions, which span BP2 to BP3 (n = 24). Together with atypical (n = 2) and unknown (n = 1) deletion classes, class I and class II deletions comprise the deletion genotype (n = 37) examined in our study. Both deletion classes encompass the $GABA_AR$ β3-α5-γ3 subunit gene cluster (i.e., GABRB3, GABRA5, and GABRG3), which is central to the interpretation of our results.

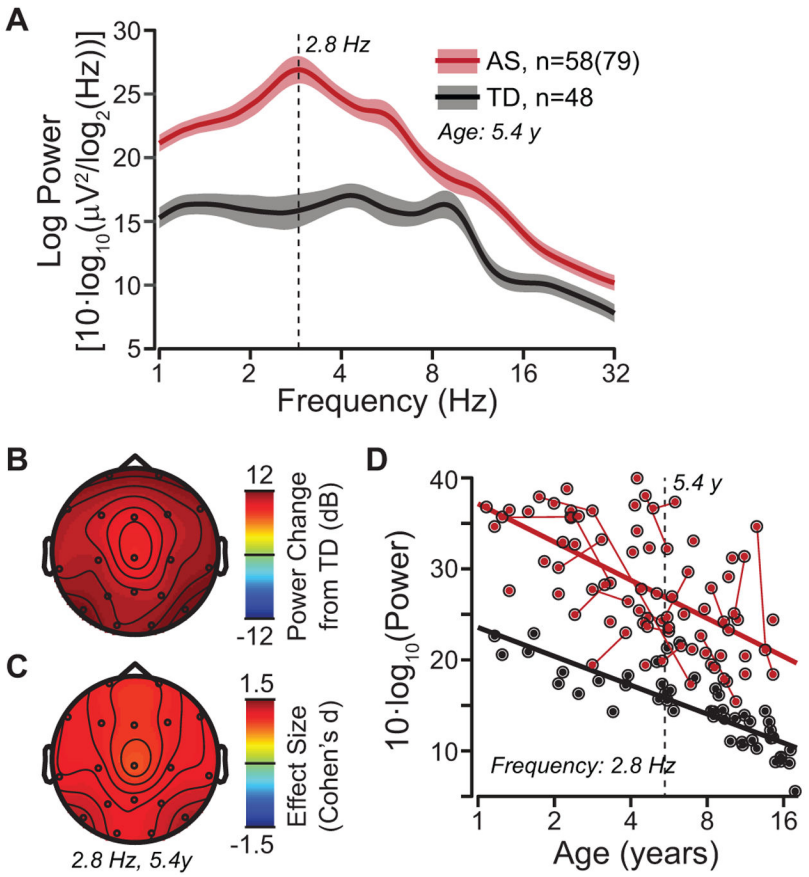

Figure 2. Spectral power differences between AS and TD controls.

(A) Grand average power spectral density derived from the LMM, with age set to the mean log age of 5.4 years (average across all visits and electrodes). AS: red, TD controls: black. The colored bands show 95% confidence intervals. (B,C) Scalp topography of power change in dB and effect size (Cohen's d) between AS and TD controls derived from the LMM for 2.8 Hz (i.e., AS delta peak frequency) and the mean log age of 5.4 years. (D) Developmental trajectory of channel averaged delta power (2.8 Hz) derived from the LMM. Longitudinal visits are connected by solid lines.

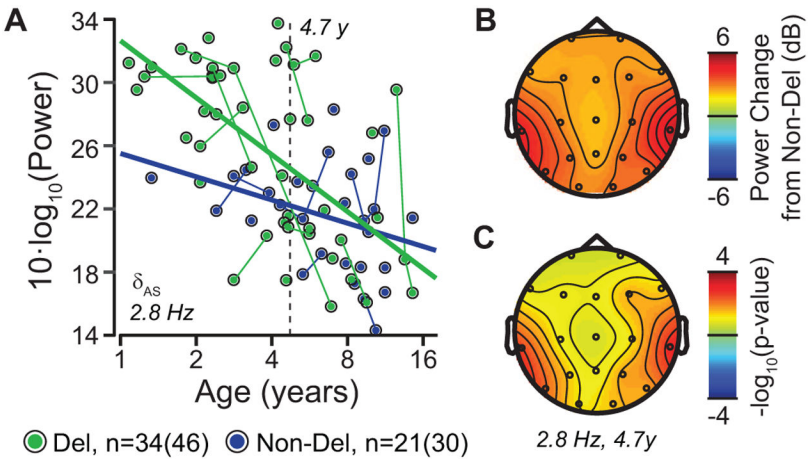

Figure 3. Spectral power in delta frequency band differs between AS genotypes.

(A) Developmental trajectory of electrode averaged delta power (2.8 Hz) derived from the LMM (average across all electrodes). Deletion AS: green, Non-deletion AS: blue. Longitudinal visits are connected by solid lines. (B,C) Scalp topography of power change in dB and p-values for t-tests between deletion AS and non-deletion AS derived from the LMM for 2.8 Hz and the mean log age of 4.7 years.

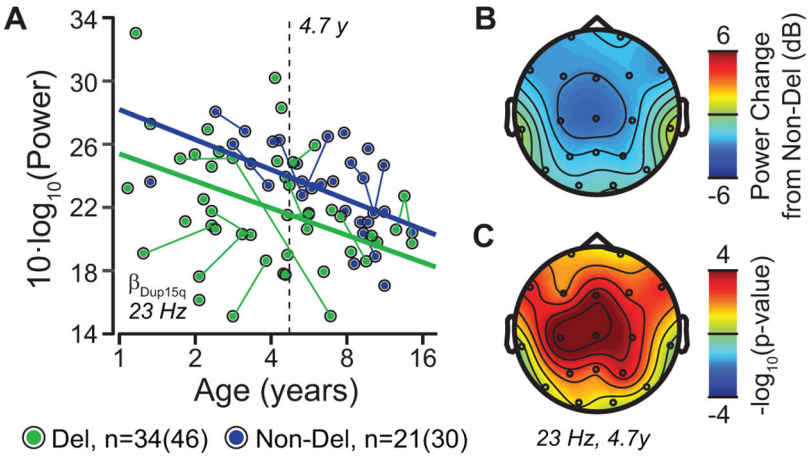

Figure 4. Spectral power in beta frequency band differs between AS genotypes.

(A) Developmental trajectory of electrode averaged beta power (23 Hz according to hypothesis 2, i.e. peak frequency derived from Dup15q syndrome EEG phenotype, (35)) derived from the LMM (average across all electrodes). Deletion AS: green, Non-deletion AS: blue. Longitudinal visits are connected by solid lines. (B,C) Scalp topography of power change in dB and p-values for t-tests between deletion AS and non-deletion AS derived from the LMM for 23 Hz and the mean log age of 4.7 years

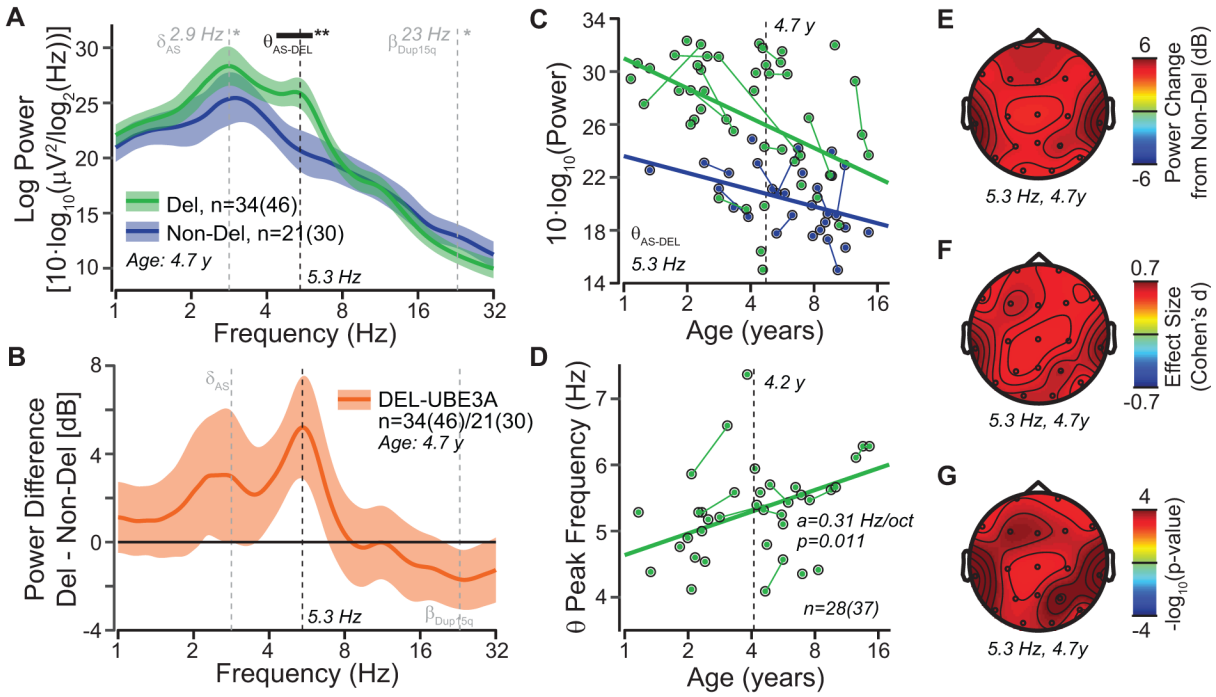

Figure 5. Spectral power differs between AS genotypes.

(A) Grand average power spectral density derived from the LMM with age set to the mean log age of 4.7 years (average across all visits and electrodes). Deletion AS: green, non-deletion AS: blue. The colored bands show 95% confidence intervals. The black bar indicates frequency ranges with significant group differences (corrected for multiple testing across frequencies). The gray lines indicate the specific hypotheses tested in the delta and beta bands (see Figures 3 and 4). (B) Difference in spectral power between deletion AS and non-deletion AS. The colored bands show 95% confidence intervals. (C) Developmental trajectory of theta power (5.3 Hz) derived from the LMM (average across all electrodes). Longitudinal visits are connected by solid lines. (D) Correlation between theta peak frequency and age. Longitudinal visits are connected by solid lines. (E-G) Scalp topography of power change in dB, effect size (Cohen's d) and p-values for t-tests between deletion AS and non-deletion AS derived from the LMM for 5.3 Hz and the mean log age of 4.7 years.

Table 1.

Medication overview. This table summarizes the proportion of non-deletion AS and deletion AS participants on each of 6 different medications types: CNS: Central Nervous System; AED: Antiepileptic Drug; AP: Antipsychotic; CSE: CNS Side Effects; AA: Alpha Agonist; STM: Stimulant. Proportions are calculated from the number of unique participants in a group taking the medication at one or more EEG recording sessions used in the analysis. Number of affected participants and EEG recordings are reported in separate columns. Test statistics and p-values from chi-squared tests are reported in the last two columns.

Drug type	Non-del Participants (%)	Non-del Participants (#)	Non-del Recordings (#)	Deletion Participant (%)	Deletion Participant (#)	Deletion Recording (#)	Chi-Square	P-value
CNS	76.2	16	23	76	28	39	1.939	0.965
AED	52.4	11	17	70	26	36	1.856	0.173
AP	9.5	2	2	3	1	2	1.271	0.260
CSE	23.8	5	7	19	7	11	0.195	0.659
AA	14.3	3	4	8	3	5	0.551	0.458
STM	4.8	1	1	0	0	0	1.793	0.181